European Drag Reduction and Flow Control Meeting – EDRFCM 2015
March 23–26, 2015, Cambridge, UK

NUMERICAL STUDY OF REDUCING TURBULENT SKIN-FRICTION DRAG USING DBD PLASMA ACTUATORS

Qiang Yang, Yongmann M. Chung
School of Engineering and Centre for Scientific Computing, University of Warwick, CV4 7AL, Coventry, UK

INTRODUCTION

Spanwise wall oscillation [4] and spanwise travelling wave by spanwise Lorentz force [2] can achieve a significant amount of skin-friction drag reduction in turbulent flow. However, the wall motion and Lorentz actuator have their own drawbacks. For example, wall movement needs mechanical components into the system, and the response frequency is quite limited; while for Lorentz actuator, it is quite heavy and the fluid must be electric conductive, *e.g.*, sea water. The DBD (dielectric barrier discharge) plasma actuator is a new type of actuator and was first used for flow control by Roth *et al.* [5]. It is simply constructed by a lower electrode and an upper electrode separated by the dielectric. Figure 1 shows two types of DBD plasma actuators, as studied by Choi *et al.* [1]. The L type actuator can generate a uni-direction plasma force while the Π type actuator can generate a bi-direction plasma force. Choi *et al.* [1] studied spanwise travelling wave and spanwise oscillation in a turbulent boundary layer by using these two types of plasma actuators. However, due to the measurement difficulty in experiment, the actual skin-friction drag reduction was not reported. In the current work, a general plasma actuator model is developed to represent the L and Π types plasma actuators; then the spanwise travelling wave and spanwise oscillation are numerically studied in a turbulent channel flow for drag reduction.

METHODOLOGY

The plasma actuator force can be obtained by solving the inverse problem of the Navier-Stokes equations using the PIV (particle image velocimetry) experimental data. The wall normal component of the plasma force f_y is usually much smaller than the tangential component f_x, thus the wall normal plasma force f_y is ignored in the present model. With this assumption, the two momentum equations are closed for solving the plasma force f_x and pressure p. Based on the plasma force f_x obtained for PIV data, we further propose the force distributions for f_x: a Rayleigh distribution in the tangential direction, *i.e.*, $\frac{x}{\sigma^2}e^{-x^2/2\sigma^2}$, and an exponential distribution in the wall normal direction, *i.e.*, $\lambda e^{-\lambda y}$. The plasma force can be written as equation 1, where I is the force strength.

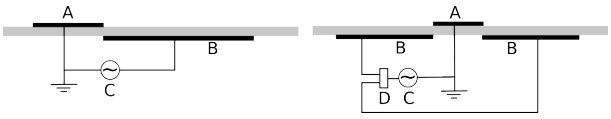

Figure 1: Schematic of the L type (left) and Π type (right) plasma actuators. A is the upper electrode; B is the lower electrode; C is the AC power source and D is the phase controller.

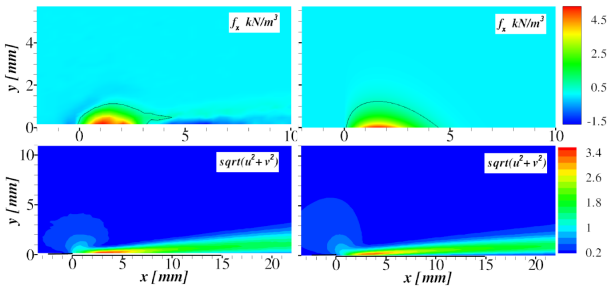

Figure 2: Comparison of the plasma force distribution (top), jet velocity (bottom) between PIV data (left) and the data from present plasma model (right).

$$f_x(x,y) = I\frac{\lambda x}{\sigma^2}e^{-x^2/2\sigma^2-\lambda y}, (x \geq 0, y \geq 0). \qquad (1)$$

Within this model, the total plasma force in the whole region is I, and the maximum plasma force $A = I\frac{\lambda}{\sigma}e^{-1/2}$ appears at the location $(\sigma, 0)$. The plasma actuator model is determined by three parameters, *i.e.*, A, σ and λ. A comparison of the plasma force distribution and the jet velocity between the PIV data and the result from the present model with $A = 5.2$, $\sigma = 1.6$ and $\lambda = 1.9$ is shown in figure 2.

The single plasma actuator modules are then arranged to be aligned in the streamwise direction on the top and bottom walls of a turbulent channel at $Re_\tau = 200$. The streamwise mass flow rate is kept constant by dynamically adjusting the streamwise mean pressure gradient. The Navier-Stokes equations are solved by using an in-house finite volume code [3]. The parameters for the plasma actuators are set as $A = 1$ (non-dimensionalised by U_m^2/h), $\sigma = 0.07$ and $\lambda = 45$, which gives a penetration depth of $\Delta^+ = 4.5$ in the present flow. The gap between the two adjacent plasma actuators is $s^+ = 50$. The maximum displacement of the plasma actuators is $D_m = 2\pi$ for all the oscillation cases.

Six configurations are considered for spanwise travelling wave and spanwise oscillation by using L type and Π type actuators. These are shown in table 1.

RESULTS

Figure 3 shows the time history of the normalised skin-friction coefficient C_f for all six configurations. Drag reduction ($\mathcal{DR}$) is obtained for C1, C2 and C6; while drag increase ($\mathcal{DI}$) for the other configurations. C1, C2 and C6 have very similar $\mathcal{DR}$ values at around 15%. The response time of C_f is very long for L type actuator with either spanwise travelling wave or spanwise oscillation. But the long term C_f is not sensitive to neither the spanwise travelling wave speed c^+

Table 1: Configurations for spanwise travelling wave (ST) and spanwise oscillation (SO).

Config.	Type	Form	Sketch
C1	L	ST	
C2	L	SO	
C3	Π	ST	
C4	Π	SO	
C5	Π	SO	
C6	Π	SO	

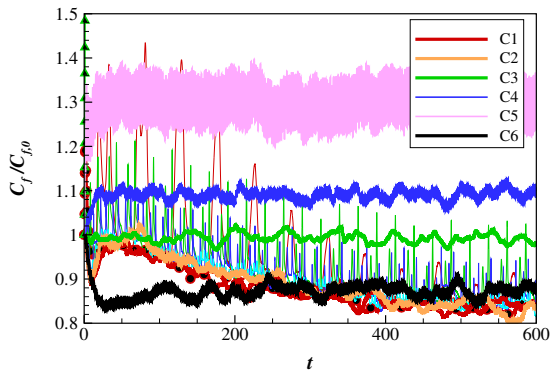

Figure 3: Normalised skin-friction coefficient C_f for all six configurations.

nor the spanwise oscillation frequency ω^+. As can see, for C1, the trajectories of C_f with $c^+ = 4$ (red line) and $c^+ = 0$ (red line with circles) are almost identical. For C2, five oscillation frequencies are considered, *i.e.*, $\omega^+ = 0.01$ (red thin line), $\omega^+ = 0.02$ (green thin line), $\omega^+ = 0.03$ (blue thin line), $\omega^+ = 0.06$ (light blue thin line) and $\omega^+ = 0.12$ (orange bold line), and the lower bound of C_f trajectories all follow that of C1. This means that for L type actuator, the simplest configuration is a stationary wave with $c^+ = 0$. Π type actuator seems to be not as successful as L type actuator in drag reduction, because majority of the configurations with Π type actuators have $\mathcal{DI}$, except C6. For C6, the skin friction decreases to a steady level very quickly, which means that the starting vortices by the plasma actuators are diminished very effectively.

The spanwise mean velocity profiles are shown in figure 4 for all six configurations. C1 and C2 generate very strong uni-direction spanwise velocity and the effect of the spanwise travelling wave and the spanwise oscillation is very small. The spanwise mean velocity for C3 nad C4 are small due to the symmetry of the plasma force. The unsteady spanwise mean velocity profiles are very similar for C5 and C6, but it is interesting to notice that these two configurations give a drag increase and reduction, respectively.

Figure 5 shows the near wall streamwise velocity streaks

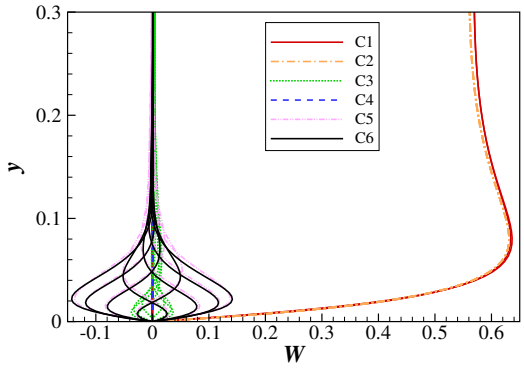

Figure 4: Spanwise mean velocity profiles for all six configurations.

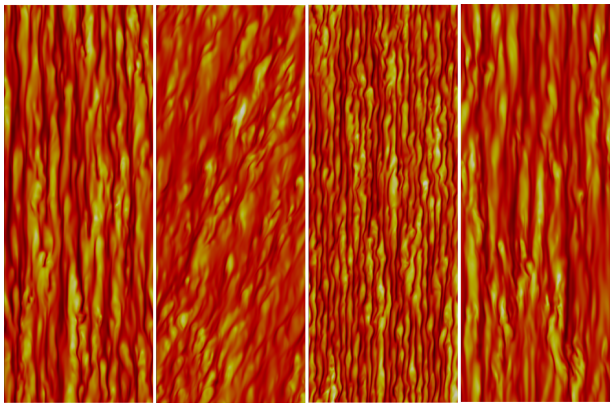

Figure 5: Streamwise velocity streaks at $y^+ = 10$ for no control case, C1, C5 and C6. Colour range is from -0.5 to 0.5.

at $y^+ = 10$ for no control case, C1, C5 and C6 after the flows are settled down. It suggests how the plasma actuators interact with the near wall low- and high-speed streaks. L type actuator can twist the streaks to one direction and break them up; Π type actuator with C5 can enhance the streaks by the local starting vortices induced by the unsteady plasma force; but Π type actuator with C6 can mix the low- and high-speed streaks, resulting in the weakening of the streaks strength.

In the conference, detailed analysis of the conditioned turbulent statistics and structures for C1 and C6 will be presented to address the drag reduction mechanism. The effect of maximum plasma force strength A, plasma actuator gap s and maximum plasma actuator displacement D_m will be discussed as well.

REFERENCES

[1] K.-S. Choi, T. Jukes, and R. Whalley. *Philosophical Transactions of the Royal Society A*, 369:1443–1458, 2011.

[2] Y. Du, V. Symeonidis, and G. E. Karniadakis. *Journal of Fluid Mechanics*, 457:1–34, 2002.

[3] E. Hurst, Q. Yang, and Y. M. Chung. *Journal of Fluid Mechanics*, 759:28–55, 2014.

[4] W. J. Jung, N. Mangiavacchi, and R. Akhavan. *Physics of Fluids A*, 4(8):1605–1607, 1992.

[5] J. R. Roth, D. M. Sherman, and S. P. Wilkinson. *AIAA Journal*, 38(7):1166–1172, 2000.